



|                                     |   |
|-------------------------------------|---|
| <b>Title</b>                        | The effect of C(s) on the trapping of NO <sub>x</sub> onto Pt/Ba/Al <sub>2</sub> O <sub>3</sub> catalysts   |
| <b>Authors(s)</b>                   | Sullivan, James A., Dulgheru, Petrica   |
| <b>Publication date</b>             | 2010-08   |
| <b>Publication information</b>      | Sullivan, James A., and Petrica Dulgheru. "The Effect of C(s) on the Trapping of NO <sub>x</sub> onto Pt/Ba/Al <sub>2</sub> O <sub>3</sub> Catalysts." Elsevier, August 2010. <a href="https://doi.org/10.1016/j.apcatb.2010.06.025">https://doi.org/10.1016/j.apcatb.2010.06.025</a> .   |
| <b>Publisher</b>                    | Elsevier  |
| <b>Item record/more information</b> | <a href="http://hdl.handle.net/10197/3993">http://hdl.handle.net/10197/3993</a>   |
| <b>Publisher's statement</b>        | This is the author's version of a work that was accepted for publication in Applied Catalysis B: Environmental. Changes resulting from the publishing process, such as peer review, editing, corrections, structural formatting, and other quality control mechanisms may not be reflected in this document. Changes may have been made to this work since it was submitted for publication. A definitive version was subsequently published in Applied Catalysis B: Environmental, 99 (1 - 2) 2010-08, pp.235-241. DOI: 10.1016/j.apcatb.2010.06.025 |
| <b>Publisher's version (DOI)</b>    | <a href="https://doi.org/10.1016/j.apcatb.2010.06.025">10.1016/j.apcatb.2010.06.025</a>   |

Downloaded 2025-12-04 23:06:08

The UCD community has made this article openly available. Please share how this access benefits you. Your story matters! (@ucd\_oa)



© Some rights reserved. For more information

## The effect of $C_{(s)}$ on the trapping of $NO_x$ onto Pt Ba $Al_2O_3$ catalysts

James A Sullivan\* and Petrica Dulgheru,  
UCD School of Chemistry and Chemical Biology  
SFI SRC in Solar Energy Conversion,  
Belfield  
Dublin 4,  
Ireland

[James.Sullivan@ucd.ie](mailto:James.Sullivan@ucd.ie)

### Abstract

Pt / BaO /  $Al_2O_3$  catalysts react with  $NO/O_2$  mixtures to form barium nitrites and nitrates. In the presence of small amounts of  $C_{(s)}$  admixed with the catalyst the concentrations of  $NO_x$  adsorbed is considerably reduced and the stability of the stored  $NO_x$  is decreased. These results suggest that there are important implications for any attempts to combine NSR and particulate combustion systems within a single catalytic system. Furthermore, it is clear that there are significant concentrations of mobile  $NO_x$  species present in the environs of the  $NO_x$  trap prior to fixation on BaO, *i.e.* the transfer between  $NO_2$  formed on the Pt component of the trap and the “fixed”  $NO_x$  in  $Ba(NO_3)_2$  involves significant concentrations of gaseous or surface mobile  $NO_2$ .

**Keywords:**  $NO_x$  trap, Particulate combustion, 4-way catalysis

### Introduction

$NO_x$  and Particulate Matter (PM) are two of the more intractable pollutants emitted from diesel engine exhausts [1-3].  $NO_x$  contributes to photochemical smog and acid rain while PM can be carcinogenic and also contributes to global warming through decreasing the albedo of Arctic and Antarctic ice. Neither is removed from the exhaust stream using conventional three way catalysts and other technologies are required.

Currently within exhaust gases of a net oxidising nature,  $\text{NO}_x$  is reduced to  $\text{N}_2$  using  $\text{NO}_x$  Storage and Reduction (NSR) technology where NO is trapped on BaO forming  $\text{Ba}((\text{NO})_3)_2$ . Once the trap is saturated a pulse of hydrocarbons over the material reacts to release NO, regenerate the BaO sorbent material and reduce the NO to  $\text{N}_2$  [4-10]. The first step in this cycle is the oxidation of NO (over Pt) to form  $\text{NO}_2$  [11, 12].

Removal of particulates can take place in a somewhat related system (the Diesel Particulate Filter – DPF) where particles are trapped in the pores of adapted monoliths. These have alternate ends plugged forcing the exhaust gas through the walls of the monolith where larger particles are trapped [13-15]. In the case of continuous regeneration systems, trapped particles are burned off using either a periodic high temperature oxidation in air or through a lower temperature reaction with  $\text{NO}_2$ .

In the latter case NO, present in the exhaust gas (in combination with a suitable NO oxidation catalyst), promotes soot combustion through the formation of  $\text{NO}_2$  which then reacts with  $\text{C}_{(s)}$  transferring an O atom and regenerating NO [16-17]

Since the oxidation of NO is a primary step both in the trapping onto an NSR material and the promotion of soot combustion on a DPF, the attempt to combine both of these technologies into a single catalytic bed seems obvious. Furthermore, it has been reported that the presence of a NSR system improves particulate removal from diesel exhausts [1, 18-20]. Previously, [21] we have shown that the reason for this improved activity is related to the increased transient concentration of  $\text{NO}_x$  present during

regeneration of the NSR material rather than to any inherent catalytic activity in the components of the NSR material.

In the same article we showed that the presence of  $C_{(s)}$  has a detrimental effect on the ability of a model Pt / BaO / SiO<sub>2</sub> material to store NO<sub>x</sub> once exposed to NO/O<sub>2</sub> mixtures at 400 °C. This obviously has an effect on the application and operation of the NO<sub>x</sub> trap in terms of the frequencies of regenerations that would be required if trap capacities fell. This in turn has an effect on the fuel efficiency of any vehicle that operates such a system.

While several groups have studied the effect of NO<sub>x</sub> (and NO<sub>x</sub> trapping materials) on soot combustion [18-23] very few have studied systematically the reverse interactions, *i.e.* the effect of soot on the activity and capacity of a NO<sub>x</sub> trap. Kustov and Makkee [23] have reported the presence of soot destabilizes NO<sub>x</sub> storage on Sr-containing NSR materials and Matarrese *at al.* [23] have reported that the presence of soot at relatively low levels (catalyst : soot ratios > 10 : 1) does not affect the trapping capacities of model Ba-containing NSR systems, while higher soot loadings (catalyst : soot = 4 : 1) do have a detrimental effect.

In the current work we study this detrimental effect of  $C_{(s)}$  on NO<sub>x</sub> storage in more detail using Al<sub>2</sub>O<sub>3</sub> supported NSR materials. Specifically, we use Al<sub>2</sub>O<sub>3</sub> to attempt to see whether the temporary storage of NO and NO<sub>2</sub> on the surface of Al<sub>2</sub>O<sub>3</sub> (a process not possible over SiO<sub>2</sub> supported materials) has any effect on the problems seen previously. We also look at the effects that (a)  $C_{(s)}$  concentrations in a catalyst-soot mixture and (b) the length of time that such mixtures are exposed to NO/O<sub>2</sub> gas

mixtures have on the concentrations and stability of adsorbed (trapped)  $\text{NO}_x$ . Transient gas switching techniques (studying the dose of  $\text{NO} + \text{O}_2$  onto the catalyst) and Temperature Programmed Desorption (studying the removal of adsorbed  $\text{NO}_x$  from the catalyst) are the tools used to probe these features. Our results concur with those reported in [23] in that the effect noted over Sr materials was reproduced here over Ba-containing materials while they contrast somewhat with [22] as in our situation the presence of even minor amounts of soot (catalyst : soot ratio = 50 : 1) have a dramatic effect on the  $\text{NO}_x$  storage capacities.

## **Experimental**

### *Catalyst Preparation*

The catalyst used in this study was a 1% Pt / 10% BaO /  $\text{Al}_2\text{O}_3$  material. The Pt precursor was a Pt acetylacetonate (acac),  $\text{Pt}(\text{CH}_3\text{COCHCOCH}_3)_2$  while the BaO was derived from barium acetate. Both salts were provided by Aldrich.  $\gamma$   $\text{Al}_2\text{O}_3$  supports were provided by Johnson Matthey and had a surface area of  $210 \text{ m}^2 \text{ g}^{-1}$ . The material was prepared through incipient wetness impregnation. In the first step the  $\text{Al}_2\text{O}_3$  was crushed and sieved to particle sizes 212-600  $\mu\text{m}$  before aliquots were repeatedly loaded with aqueous solutions containing sufficient barium acetate to eventually result in a 10% BaO loading. The material was dried at 80 °C before being calcined for 2h at 500 °C. Subsequently the powder was loaded with a Pt acetylacetonate (acac),  $\text{Pt}(\text{CH}_3\text{COCHCOCH}_3)_2$  solution in  $\text{CH}_3\text{NO}_2$  of sufficient concentration to result in a 1% loading. This powder was subjected to the same drying / calcination treatment as above.

Printex U (Degussa) is a commercial Carbon Black and was used as a model soot. The properties of Printex U have been previously described [24]. Catalyst soot mixtures were prepared in varying ratios as follows. The catalyst (1g 1%Pt / 10% BaO / Al<sub>2</sub>O<sub>3</sub>) was mixed with 0 - 200 mg of soot in different catalyst to soot ratios. After the required masses of catalyst and soot were weighed they were transferred to a glass vial and mixed for about 1 minute using a spatula. This approximates a loose contact situation (similar to the one in a diesel particulate filter). Accurately weighed aliquots of these mixtures were subsequently used in TPD experiments.

#### *NO/O<sub>2</sub> adsorption step and Temperature Programmed Desorption*

The catalysts (50 mg of catalyst or catalyst : soot mixture) were loaded into a tubular reactor (OD 8 mm) and held in place using two plugs of quartz wool. The mass of all catalyst : soot mixtures was chosen such that 50 mg of catalyst was present in the reactor. The reactor was placed in a furnace connected to a gas handling system. The catalyst was initially held in a flow of He (100 mL min<sup>-1</sup>) and the temperature was raised from room temperature to 400 °C. It was held at this temperature for a brief period (10 min) before the NO + O<sub>2</sub> dose commenced. The NO was taken from a certified cylinder of 1% NO/He (BOC) while the He and O<sub>2</sub> were taken from high purity O<sub>2</sub> and He cylinders also provided by BOC. The flow rates of the individual gases were controlled using Bronkhorst mass flow controllers powered by an in-house constructed power supply.

The gas handling system was designed in such a way that a He flow (100 mL min<sup>-1</sup>) over the catalyst could be replaced (through actuation of an electronically controlled valve) with a stream that contained a mixture of NO (2000 ppm), O<sub>2</sub> (10 %) and He

while retaining the same overall flow ( $100 \text{ mL min}^{-1}$ ). This mixture flowed over the catalyst for a defined amount of time (60, 300 or 600 s) before being replaced once more with the pure He stream. During these doses the catalyst was contacted with (160, 800 and  $1600 \text{ } \mu\text{mol NO g}^{-1}$  respectively). Recall that the catalyst composition used (1% Pt / 10% BaO /  $\text{Al}_2\text{O}_3$  contains  $730 \text{ } \mu\text{mol Ba g}^{-1}$  resulting in a theoretical  $\text{NO}_x$  trapping capacity assuming that all Ba atoms are available to act as a  $\text{NO}_x$  store (through the formation of  $\text{Ba}(\text{NO}_3)_2$ ) of  $1460 \text{ } \mu\text{mol NO g}^{-1}$ . During these experiments the mass spectrometer monitored fragments at  $m/z = 4, 16, 17, 18, 22, 28, 30, 32, 44$  and  $46$ . The relevant profiles were (following suitable corrections due to fragmentation overlaps) converted to units of concentration and plotted as a function of time. Specifically, regarding treatment of the NO and  $\text{NO}_2$  profiles the contribution of  $\text{NO}_2$  to the NO signal at  $m/z = 30$  was removed (through a knowledge of the cracking patterns of  $\text{NO}_2$  within the mass spectrometer [25]) before the NO signal was converted to ppm.  $\text{NO}_2$  profiles were converted to ppm through calibration plots at  $m/z = 46$ .

Comparison of  $m/z = 44$  profiles with those of  $m/z = 28$  and  $12$  suggest  $\text{N}_2$  or  $\text{N}_2\text{O}$  formation during the dose periods or subsequent TPD experiments is minimal, *i.e.* the  $m/z = 12$  and  $28$  profiles mirror that for  $m/z = 44$  (suggesting that the bulk of the signal from  $m/z = 44$  derives from  $\text{CO}_2$ ). Similarly the  $m/z = 14$  (N) signal mirrors those of  $m/z = 30$  ( $\text{NO} + \text{NO}_2$ ) and  $m/z = 46$  ( $\text{NO}_2$ ). This does not rule out the formation of minor amounts of  $\text{N}_2$  or  $\text{N}_2\text{O}$ .

At this time the reactor was cooled to  $200 \text{ }^\circ\text{C}$  in the He flow. This cooling took approximately ten minutes. After the mass spectrometer readings had returned to the

baseline values the TPD protocol was commenced. The temperature of the catalyst was ramped at a rate of  $20\text{ }^{\circ}\text{C min}^{-1}$  between  $200\text{ }^{\circ}\text{C}$  and  $750\text{ }^{\circ}\text{C}$  while the exit gases were continuously monitored by Mass Spectrometry (Prolab) and the fragments at  $m/z = 4, 16, 17, 18, 22, 28, 30, 32, 44$  and  $46$  were recorded. As above, the outputs were converted into concentration units and plotted in TPD profiles as a function of temperature.

## Results and Discussion

Figure 1 shows the  $\text{NO}$ ,  $\text{NO}_2$  and  $\text{NO}_x$  profiles measured at the exit of the reactor during different exposures ( $60\text{ s}$ ,  $300\text{ s}$  and  $600\text{ s}$ ) of  $1\% \text{ Pt} / 10\% \text{ BaO} / \text{Al}_2\text{O}_3$  catalyst to  $\text{NO} + \text{O}_2$  mixtures at  $400\text{ }^{\circ}\text{C}$ . The  $\text{NO} + \text{O}_2$  mixture is switched into the reactor at 1 minute and removed at 2, 6 and 11 minutes respectively. The profiles relating to the  $60\text{ s}$  dose are the lower three, the  $300\text{ s}$  dose the middle three and the  $600\text{ s}$  dose the upper 3 curves.

It is clear that only a very small amount of  $\text{NO}_x$  leaves the reactor during the first minute of the dose, *i.e.* the vast majority of the incoming  $\text{NO}_x$  is trapped on the catalyst. Following this, breakthrough takes place and  $\text{NO}$  and  $\text{NO}_2$  ( $\text{NO}_x$ ) begins to appear in the exit stream. As expected, its concentration rises with additional time. After 5 minutes of  $\text{NO} + \text{O}_2$  dosage, the  $\text{NO}$  level is approximately  $2000\text{ ppm}$ .

When each dose is completed and the  $\text{NO} + \text{O}_2$  is removed from the stream the measured  $\text{NO}$  level (but not the  $\text{NO}_2$  level) actually increases for over 1 minute ( $\text{NO}$  was removed at minute 2, 6 and 11 of the plots) before it (and the overall  $\text{NO}_x$  level) falls back to background levels. This shows that the  $\text{NO}_x$  species adsorbed at  $400\text{ }^{\circ}\text{C}$



in the presence of NO and O<sub>2</sub> were unstable during the cooling process in the inert atmosphere. This may indicate a partial decomposition of Ba(NO<sub>3</sub>)<sub>2</sub> which is unstable in the inert atmosphere (although bulk Ba(NO<sub>3</sub>)<sub>2</sub> is stable in inert atmospheres to far higher temperatures) or to the removal of NO<sub>x</sub> species stored on the Al<sub>2</sub>O<sub>3</sub> surface. This effect, *i.e.* the release of amounts of NO<sub>x</sub> from the storage material once gaseous NO had been removed from the inlet stream has been seen before (albeit in the absence of cooling) in reference [26] and ascribed to these possibilities.

However, the fact that the NO<sub>x</sub> released is solely NO and not NO<sub>2</sub> suggests disproportionation of NO<sub>2ads</sub> to NO<sub>3ads</sub> and NO<sub>ads</sub> and this NO (being unstable on the surface at the catalyst temperature) desorbs from the surface. The generation of NO from NO<sub>2</sub> during the loading of a NO<sub>x</sub> trap has been previously seen and explained in these terms [27-30]. Another feature to note is that the subsequent TPD measurements show NO<sub>x</sub> (predominantly NO accompanied by O<sub>2</sub>) desorption commences at temperatures below the dose temperature of 400 °C (see below). This points to substantial reorganisation within the NO<sub>x</sub> adsorbed layer, *i.e.* the NO / NO<sub>2</sub> which was stable enough to remain on the surface at 400 °C and during the cooling phase had reacted in some way (during the latter) to become unstable at 400 °C.

CO<sub>2</sub> is also released from the NSR materials once they are exposed to NO + O<sub>2</sub> at 400 °C. This arises from the displacement of BaCO<sub>3</sub> during the formation of Ba(NO<sub>3</sub>)<sub>2</sub> and has been seen several times previously *e.g.* in [26]. The BaCO<sub>3</sub> arises both during the calcination of Barium acetate (where formed CO<sub>2</sub> reacts with surface BaO at high temperatures) and the adsorption of atmospheric CO<sub>2</sub> during storage of the material. A plot showing the mass spectrometer response at  $m/z = 44$  following the inlet of NO

+ O<sub>2</sub> in following a typical switch is shown in Supporting Information (S1). This also shows the  $m/z = 44$  profile from an analogous switch in the presence of C<sub>(s)</sub> – see later.

Figure 2 shows the resulting NO<sub>x</sub> TPD profiles obtained when these materials are subjected to a temperature ramp (in He) to 750 °C at a rate of 20 °C min<sup>-1</sup> after being cooled in He (to 200 °C) following the NO + O<sub>2</sub> dose. In all cases NO was the predominant form of NO<sub>x</sub> desorbed (higher profiles). Minor (unquantifiable using our analysis conditions) amounts of NO<sub>2</sub> were seen from samples (lower three profiles in Figure 2) which had been dosed for 10 minutes. These results are similar to the results seen by Nova *et al.* [26] and, in their case the lack of large amounts of NO<sub>2</sub> was ascribed to the rapid decomposition of any desorbed NO<sub>2</sub> before it left the reactor. In all cases the NO was accompanied by a release of O<sub>2</sub> (see supporting information Figure S2 for an example). At higher temperatures CO<sub>2</sub> desorption is also seen. These desorptions (shown in S3) relate to the decomposition of BaCO<sub>3</sub> and interestingly more CO<sub>2</sub> desorbs from samples which had been dosed for lower times in NO + O<sub>2</sub> – suggesting, not unreasonably, that proportionately less CO<sub>2</sub> had been desorbed from the NO<sub>x</sub> storage materials during these doses.

In the case of the sample dosed in NO + O<sub>2</sub> for 60 s the desorption of NO begins at 440 °C, reaches a maximum at 550 °C and is complete by 720 °C. In total 131 μmol g<sup>-1</sup> of NO was released during TPD. In the case of the sample dosed in NO + O<sub>2</sub> for 300 s NO begins to desorb at 350 °C, reaches a maximum at 480 °C and is complete at approximately 730 °C. During this TPD 402 μmol g<sup>-1</sup> NO are desorbed. Samples dosed in NO + O<sub>2</sub> for 600 s began to desorb NO at approximately 380 °C with the desorption reaching a maximum at 520 °C. More NO<sub>x</sub> is desorbed during this TPD

(521  $\mu\text{mol g}^{-1}$ ). The temperatures of desorption are similar to those seen previously for the decomposition of surface and bulk  $\text{Ba}(\text{NO}_3)_2$  [29, 30]. These results indicate that the initial  $\text{NO}_x$  dosed onto the catalyst “finds” very stable sites on which to adsorb (given that the temperature of maximum desorption and the initial temperature of desorption can be taken as a measures of stability) and also that most of the easily accessible sites are saturated following a 5 minute dose, *i.e.* doubling the dose time to 10 minutes increases the  $[\text{NO}_x]$  adsorbed only by approximately 25%. In terms of the proportion of BaO utilized during the  $\text{NO}_x$  trapping experiments the dose at 60 s utilizes approximately 9% of the Ba while those lasting for 300 and 600 s utilize approximately 27% and 36% respectively. This confirms that there are significant portions of BaO that are not available for  $\text{NO}_x$  trapping (presumably buried in the bulk of  $\text{BaCO}_3$  particles) and this is consistent with previous observations of  $\text{NO}_x$  trapping capacity in related model systems [2, 4, 33].

Interestingly, for both of the longer dose times desorption of NO begins at temperatures below that at which the  $\text{NO} + \text{O}_2$  dose was made. This indicates that material which remained on the surface following a dose at 400 °C were altered during the cooling phase, becoming less stable and eventually desorbed at a lower temperature than that at which they were initially held. This result, along with the desorption seen above in the absence of  $\text{NO} + \text{O}_{2(\text{g})}$  indicates a redistribution of the  $\text{NO}_x$  adsorbed onto the surface during the cooling in He between 400 and 200 °C where some less stable  $\text{NO}_x$  – containing species are formed.

The final interesting feature that should be discussed is the relative stabilities of the species remaining on the material following the doses for different times. It appears

that the first adsorbed  $\text{NO}_x$  finds the most stable sites while the  $\text{NO}_x$  adsorbed after a 5 minute dose is significantly less stable (in terms of temperature of maximum and initial NO desorption). Subsequently, following a 10 minute dose the  $\text{NO}_x$  adsorbed shows intermediate stabilities according to the  $T_{\text{max}}$  and  $T_{\text{initial}}$  criteria. This is reproducible behaviour and we ascribe the gain in stability of the  $\text{NO}_x$  adsorbed between 5 and 10 minute doses to a dynamic equilibration of the formed surface nitrates with  $\text{NO}_{(\text{g})}$ ,  $\text{O}_{2(\text{g})}$  and  $\text{NO}_{2(\text{g})}$  during the extended dose.

Figure 3 shows the NO,  $\text{NO}_2$ ,  $\text{NO}_x$  and  $\text{CO}_2$  profiles measured at the exit of the reactor during different exposures (60 s, 300 s and 600 s) of a mixture of 50 mg Pt / BaO /  $\text{Al}_2\text{O}_3$  catalyst and 5 mg of Printex U (Degussa) soot to  $\text{NO} + \text{O}_2$  at 400 °C (at the same concentrations as shown in Figure 1). The breakthrough profiles for NO /  $\text{NO}_2$  /  $\text{NO}_x$  are roughly comparable to the situations seen in the absence of soot however there are some differences in the composition of the  $\text{NO}_x$ . Here, much smaller amounts of  $\text{NO}_2$  were noted during the dose period compared to those seen during the dose periods in the absence of soot. As an example, at the end of the 600 s dose before  $\text{NO} + \text{O}_2$  is removed from the stream approximately 31% of the exit gas  $\text{NO}_x$  was  $\text{NO}_2$  while in the same experiment in the presence of soot the proportion was approximately 6%. This indicates reaction of  $\text{NO}_2$  with soot to form NO. All profiles again show the transient release of NO (not  $\text{NO}_2$ ) once the  $\text{NO} + \text{O}_2$  is removed from the stream (for the reasons outlined above) although this is a lot less pronounced than in the absence of soot.

$\text{CO}_2$  production begins immediately once  $\text{NO} + \text{O}_2$  is introduced into the stream and production ceases once  $\text{NO} + \text{O}_2$  is removed from the reactor inlet. This  $\text{CO}_2$  arises

from two sources, *i.e.* the decomposition of  $\text{BaCO}_3$  and the combustion of the  $\text{C}_{(\text{s})}$  in the catalyst soot mixture. The former source is important in the early portions of the switch (see supporting information Figure S1) but the main source of the  $\text{CO}_2$  observed following the initial decomposition of surface  $\text{BaCO}_3$  is the combustion of  $\text{C}_{(\text{s})}$ . In principle, the  $\text{CO}_2$  profile from the 300 s dose should mirror exactly the first 300 s of the 600 s dose and in fact the shapes of the profiles are the same. However it seems that more  $\text{CO}_2$  is produced in the latter experiment. This is more than likely due to inhomogeneity within the catalyst – soot mixture. In both cases a *pseudo* steady-state conversion to  $\text{CO}_2$  is reached roughly 2 minutes after the  $\text{NO} + \text{O}_2$  is switched into the stream and this gradually decreases as the time of reaction increases.

Figure 4 shows the  $\text{CO}_2$  and  $\text{NO}$  temperature programmed desorption profiles obtained from the three catalyst – soot mixtures following these difference pre-treatments in  $\text{NO} + \text{O}_2$ . There was no evidence of any measurable  $\text{N}_2$  formation through the course of any of the TPD (or  $\text{NO} + \text{O}_2$  dose) measurements (the  $\text{N}$  fragment mirrors exactly the  $\text{NO}$  signal at  $m/z = 30$ ). There was also no measureable  $\text{NO}_2$  desorption although again there were  $\text{O}_2$  desorptions accompanying the  $\text{NO}$  desorption. The first obvious feature to note is that the amount of  $\text{NO}_x$  ( $\text{NO} + \text{NO}_2$ ) desorbed is significantly decreased relative to the same catalysts dosed under the same conditions in the absence of soot. The second feature is that the temperatures of initial and maximum desorption are lower in each case also (see table 1, 4<sup>th</sup> row of data).

The  $\text{CO}_2$  profiles are also of interest during these TPD measurements.  $\text{CO}_2$  is seen from approximately the same temperature during the temperature ramp as  $\text{NO}$ . Its concentration increases with temperature (as does the concentration of  $\text{NO}$ ). However,

in the case of NO, once the surface concentration becomes the limiting factor in the development of the desorption profile, *i.e.* above  $T_{\max}$ , the gas phase concentration decreases once more. This is not the case with the CO<sub>2</sub> profile which continues to rise, showing a shoulder at approximately 550 °C and reaching a maximum at approximately 680 °C. This profile can be explained by the decomposition of different types of BaCO<sub>3</sub> on the catalyst surface [33]. We cannot rule out a contribution from the reaction between liberated O<sub>2</sub> and C<sub>(s)</sub> (which can take place as long as gas phase O<sub>2</sub> is available) however, inspection of the oxygen derived peak (which is coincident with the NO desorption) and the CO<sub>2</sub> peak (the low temperature shoulder of which is not coincident with these maxima) suggests this feature is more likely to involve a thermal decomposition of BaCO<sub>3</sub>.

This decomposition temperature is similar to those seen previously for the decomposition of surface BaCO<sub>3</sub> species [28-30]. There are two possible sources for the formation of this BaCO<sub>3</sub>, *i.e.* atmospheric CO<sub>2</sub> picked up during or after the preparation of the catalyst, or CO<sub>2</sub> formed during the dose of the catalyst – soot mixture at 400 °C in NO + O<sub>2</sub>. Comparisons of the CO<sub>2</sub> profiles shown here (following the dose in the presence of soot) with those seen during TPD of catalysts dosed with NO + O<sub>2</sub> in the absence of soot (supporting information Figure S3) suggest that significant portions of the decomposing BaCO<sub>3</sub> is formed from a BaO + CO<sub>2</sub> reaction at 400 °C during the dose in NO + O<sub>2</sub> where the CO<sub>2</sub> is formed from the oxidation of C<sub>(s)</sub> at this temperature, *i.e.* CO<sub>2</sub> profiles seen during the TPD of NO<sub>x</sub> from catalysts dosed in the absence of soot are lower than in Figure 4 above.

The effect of  $[C_{(s)}]$  was also studied and experiments were carried out where 50 mg of catalyst was mixed with different masses of  $C_{(s)}$  ranging from 1 mg to 10 mg (resulting in catalyst : soot ratios of between 50:1 and 5:1. Table 1 compares the absolute amounts of  $NO_x$  desorbed and the temperature of maximum desorption for each experiment in the absence and the presence of 0 - 10 mg of soot (catalyst : soot ratios of between  $\infty$  and 5 : 1). In all cases the absolute amount of  $NO_x$  desorbed is much decreased and the temperature of initial and maximum desorption falls in the presence of soot.

Figure 5 shows the  $NO$ ,  $NO_2$  and  $CO_2$  profiles seen during a 300 s dose of the catalyst in  $NO + O_2$  in the presence of varying (1 mg, 2.5 mg, 5 mg and 10 mg) amounts of  $C_{(s)}$  (the  $NO_x$  profiles ( $NO + NO_2$ ) have been left out for clarity) while Figure 6 shows the  $CO_2$  and  $NO$  TPD profiles following this dose (again no  $NO_2$  was noted during the TPD experiments). For reference in Figure 5 the  $NO$ ,  $NO_2$  and  $CO_2$  profiles relating to the 300 s dose of  $NO + O_2$  onto the catalyst in the absence of  $C_{(s)}$  are also shown. For reasons of clarity the respective TPD profiles from the latter experiment are not shown in Figure 6.

From the profiles in Figure 5 it is clear that the different concentrations of soot have a relatively small effect on the  $NO_x$  adsorption behaviour. Roughly equivalent  $NO$  breakthrough profiles are noted over 50 mg of catalyst mixed with 1, 2.5, 5 and 10 mg of soot. There is no correlation with this breakthrough time or levels and the amount of soot in the mixture, *i.e.* the shapes of the profiles are similar when 1mg or 10 mg are admixed with the 50 mg of 1% Pt / 10% BaO /  $Al_2O_3$ . At the completion of the 300s dose, once the  $NO + O_2$  is removed there is, in all cases, a relatively small

release of NO (not NO<sub>2</sub>) from the catalyst and this is the same (although noticeably smaller) feature that was seen in Figure 1 in the absence of C<sub>(s)</sub>.

As before (Figure 3) in the presence of soot the levels of NO<sub>2</sub> in the NO<sub>x</sub> mixture are far lower than when soot is absent. At the end of a 5 minute dose in the absence of soot 18 % of the NO<sub>x</sub> is NO<sub>2</sub> while in the presence of the various amounts of C<sub>(s)</sub> this falls to approximately 6 %. This is due to the reaction of any formed NO<sub>2</sub> with C<sub>(s)</sub> and subsequent reformation of NO. There is no systematic relationship between the levels of C<sub>(s)</sub> in the reaction mixture and the levels of NO<sub>2</sub> in the exhaust gas leaving the reactor.

As expected, the CO<sub>2</sub> profiles seen during the dose of the catalyst – soot mixtures in the presence of different levels of soot do differ in a systematic way from one another. In all cases the production of CO<sub>2</sub> begins once the NO + O<sub>2</sub> is switched into the stream, reaches a pseudo-steady state production after approximately 90 s and ceases as the NO + O<sub>2</sub> is removed from the stream. The amounts of CO<sub>2</sub> produced during each experiment varies as a direct function of the amount of C<sub>(s)</sub> in the catalyst soot mixture with most being produced when the catalyst soot ratio is 5:1 (10 mg soot) and least when this is 50:1 (1 mg soot). For reference the CO<sub>2</sub> profile from the initial dose of NO + O<sub>2</sub> onto the catalyst in the absence of soot is also shown (!). This confirms that a significant amount of the CO<sub>2</sub> released during the early part of the dose derives from the decomposition of surface BaCO<sub>3</sub> rather than the combustion of C<sub>(s)</sub>. The importance of this contribution obviously decreases with time as the surface [BaCO<sub>3</sub>] which can be displaced in this way is depleted.



The NO and CO<sub>2</sub> profiles recorded during the related TPD experiments are shown in Figure 6 (No NO<sub>2</sub> was noted during the TPD although again in all cases O<sub>2</sub> desorbed with the same profile as NO). There is no direct correlation between the concentration of soot present in the catalyst – soot admixture and the amount of NO desorbed. While the least amount of NO is desorbed from the 5:1 catalyst – soot mixture (containing 10 mg soot with 50 mg catalyst) the most NO (within the 4 profiles being compared here) is desorbed from the admixture containing 2.5 mg soot (catalyst:soot ratio of 20:1). The maximum temperature of desorption during these experiments ranged from 445 °C to 470 °C (recall, in the absence of soot the maximum temperature of desorption following a 300 s dose was centred at 480 °C).

On the other hand, the extent of the evolved CO<sub>2</sub> profiles again directly follow the concentrations of soot in the catalyst – soot mixtures with the most CO<sub>2</sub> seen from the 5:1 catalyst soot mixture and the least from the 50:1 mixture. The CO<sub>2</sub> profiles all follow the same shape as seen previously, *i.e.* two desorptions relating to the decomposition of different types of surface BaCO<sub>3</sub>. While the contribution of liberated O<sub>2</sub> + C<sub>(s)</sub> cannot be ruled out for the lower temperature formation of CO<sub>2</sub> the shapes of the profiles indicate that any contribution of this reaction is relatively minor, *i.e.* the NO / O<sub>2</sub> profiles peak at different temperatures to the first CO<sub>2</sub> shoulder.

Table 1 shows the amounts of NO<sub>x</sub> desorbed from the TPD experiments as a function of dose times and soot concentrations. The nominal proportion of BaO used in storing the NO<sub>x</sub> is also shown, although it should be noted that this assumes that all the Ba is present as BaO and available to trap NO<sub>x</sub> – a situation we know not to be the case. Nevertheless it provides a useful comparison of the relative amounts of NO<sub>x</sub> trapped.

It is clear both from the Table and the plots in Figure 6 that, in the presence of soot, the amount of  $\text{NO}_x$  that this model NSR system can trap is much decreased in the presence of  $\text{C}_{(s)}$  and the adsorbed  $\text{NO}_x$  is less stable (as measured by the temperatures of initial and maximum desorption). The latter feature is particularly noticeable when comparing data from the 60 s and 600 s doses and is somewhat less pronounced when the 300 s data is compared. Recall that the  $\text{NO}_x$  adsorbed in the absence of soot for 300 s was less stable than that adsorbed at 60 s (where the most stable sites are populated) or at 600 s (where we ascribe an increased stability to an extended equilibration between adsorbed  $\text{NO}_x$  and gas phase NO).

The effect of  $\text{C}_{(s)}$  in altering the stability of stored  $\text{NO}_x$  has been noted previously [23] on a Sr-containing  $\text{NO}_x$  storage system. The reason for this probably relates to surface reactions between  $\text{C}_{(s)}$  and stored nitrates. These redox reactions would form adsorbed nitrites which would be less stable and therefore decompose at lower temperatures.

The former result, *i.e.* where soot has such a detrimental effect on  $\text{NO}_x$  adsorption on a model Pt / BaO /  $\text{Al}_2\text{O}_3$  catalysts have been reported previously by Matarrese *et al.* [22], but only when lower catalyst soot ratios have been used. These workers noted no impairment of  $\text{NO}_x$  trapping capacity when catalyst soot ratios in the range 49:1 to 9:1 have been used, and a decrease in capacity at very high soot loading (catalyst soot ratios of 4:1). In contrast, the experiments here detail cases where  $\text{NO}_x$  trapping is significantly impaired in systems with catalyst : soot ratios as low as 50 : 1.

We ascribe these conflicting results to the fact that the doses of NO +  $\text{O}_2$  onto the catalyst soot mixture in this work were carried out at 400 °C while they were carried

out at 350 °C in the cited work. In that case the rate of NO<sub>2</sub> assisted soot combustion would be lower. Reference [21] shows (albeit comparing T= 300 °C and 400 °C) an order of magnitude increase in the production of CO<sub>2</sub> from NO<sub>2</sub> promoted soot oxidation (where the NO<sub>2</sub> is formed *in situ* from the oxidation of NO) between these two temperatures. Therefore in the case of the work of Matarrese *et al.* less formed NO<sub>2</sub> would react with C<sub>(s)</sub>, allowing a greater proportion of the NO<sub>2</sub> to adsorb, react and form stored nitrates. Therefore, the presence of soot would have a lesser impact on NO<sub>x</sub> adsorption.

## Conclusions

In the presence of even small masses of C<sub>(s)</sub> the amounts of NO<sub>x</sub> that a NO<sub>x</sub> trap can store in the presence of NO + O<sub>2</sub> at 400 °C is decreased considerably. A proposed reason for this is that NO<sub>2</sub> formed on Pt from the NO + O<sub>2</sub> reaction is reduced to NO through reaction with soot before it is able to react with BaO and form stable Ba(NO<sub>3</sub>)<sub>2</sub>. A schematic of the proposed mechanism is shown in Scheme 1. The amount of NO<sub>x</sub> trapped is not grossly affected by the mass of soot in the catalyst : soot mixture with no systematic change in NO<sub>x ads</sub> levels when catalyst : soot ratios are changed between 50:1 and 5:1.

The adsorbed NO<sub>x</sub> also appears to be somewhat less stable (in terms of T<sub>initial</sub> and T<sub>max</sub> of the evolved NO TPD profiles) in the presence of soot. We ascribe this to any NO<sub>x</sub> adsorbed close to a C<sub>(s)</sub> particle reacting as the temperature is raised, thereby getting reduced to less stable NO-containing species and desorbing.

One final feature of interest is the fact that this decreased trapping efficiency effect is very pronounced even at very low levels of C<sub>(s)</sub> in the catalyst : soot mixture, *e.g.* for a

sample dosed for 600 s in  $\text{NO} + \text{O}_2$  the trapping efficiency goes from roughly 35 % to approximately 9% when 1 mg of soot is added to the catalyst (a 50:1 catalyst : soot ratio). It is not possible, at these low levels of soot, for the soot particles to be in intimate (or even close) proximity to all the BaO available. Visually the mixture is clearly heterogeneous with white catalyst particles being prevalent and discrete black soot particles spread through the catalyst bed. The fact that this small amount of soot which is not in intimate contact with the BaO has such a dramatic effect on the concentration of stored  $\text{NO}_x$  suggests that there is considerable (either gas phase or surface) mobility in the  $\text{NO}_2$  generated on the Pt particles before fixation into  $\text{Ba}(\text{NO}_3)_2$  takes place. This in turn suggests that significant amounts of the  $\text{NO}_x$  trapping process does not involve a straightforward spill-over of  $\text{NO}_2$  from Pt particles to BaO.

### **Acknowledgements**

We gratefully acknowledge funding from EPA Ireland under the STRIVE programme and fellowship funding from the Roberto Rocca Education Program to support PD.

### **References**

- [1] L. Castoldi, R. Matarrese, L. Lietti, P. Forzatti, Applied Catalysis B-Environmental 64 (2006) 25-34.
- [2] M. Piacentini, M. Maciejewski, A. Baiker, Applied Catalysis B-Environmental 60 (2005) 265-275.

- [3] A. Setiabudi, M. Makkee, J.A. Moulijn, *Applied Catalysis B-Environmental* 42 (2003) 35-45.
- [4] J. Oi, A. Obuchi, G.R. Bamwenda, A. Ogata, H. Yagita, S. Kushiya, K. Mizuno, *Applied Catalysis B-Environmental* 12 (1997) 277-286.
- [5] G.R. Bamwenda, A. Obuchi, A. Ogata, J. Oi, S. Kushiya, K. Mizuno, *Journal of Molecular Catalysis A-Chemical* 126 (1997) 151-159.
- [6] M. Piacentini, M. Maciejewski, A. Baiker, *Topics in Catalysis* 42-43 (2007) 55-59.
- [7] A. Casapu, J.D. Grunwaldt, M. Maciejewski, F. Krumeich, A. Baiker, M. Wittrock, S. Eckhoff, *Applied Catalysis B-Environmental* 78 (2008) 288-300.
- [8] I. Nova, L. Lietti, P. Forzatti, *Catalysis Today* 136 (2008) 128-135.
- [9] L. Olsson, P. Jozsa, M. Nilsson, E. Jobson, *Topics in Catalysis* 42-43 (2007) 95-98.
- [10] K. Shimizu, Y. Saito, T. Nobukawa, N. Miyoshi, A. Satsuma, *Catalysis Today* 139 (2008) 24-28.
- [11] I. Nova, L. Castoldi, F. Prinetto, V. Dal Santo, L. Lietti, E. Tronconi, P. Forzatti, G. Ghiotti, R. Psaro, S. Recchia, *Topics in Catalysis* 30-31 (2004) 181-186.
- [12] B.R. Kromer, L. Cao, L. Cumarantunge, S.S. Mulla, J.L. Ratts, A. Yezerets, N.W. Currier, F.H. Ribeiro, W.N. Delgass, J.M. Caruthers, *Catalysis Today* 136 (2008) 93-103.
- [13] U. Hoffmann, T. Rieckmann, J.X. Ma, *Chemical Engineering Science* 46 (1991) 1101-1113.

- [14] B.A.A.L. van Setten, M. Makkee, J.A. Moulijn, *Catalysis Reviews-Science and Engineering* 43 (2001) 489-564.
- [15] P. Ciambelli, P. Corbo, V. Palma, P. Russo, S. Vaccaro, B. Vaglieco, *Topics in Catalysis* 16 (2001) 279-284.
- [16] J.A. Sullivan, O. Keane O and L. Maguire, *Catal. Comm.* 6, (2005) pp 472-475.
- [17] J.A. Sullivan and O. Keane *Catal. Today*, 114, (2006), 340-345.
- [18] K. Krishna, M. Makkee, *Catalysis Today* 114 (2006) 48-56.
- [19] B.R. Stanmore, J.F. Brilhac, P. Gilot, *Carbon* 39 (2001) 2247-2268.
- [20] A. Setiabudi, M. Makkee, J.A. Moulijn, *Applied Catalysis B-Environmental* 50 (2004) 185-194.
- [21] J.A. Sullivan, O. Keane, A. Cassidy, *Applied Catalysis B: Environmental* 75, (2007), 102-106
- [22] R. Matarrese, L.Castadoldi, L.Lietti, P.Forzatti, *Topics in Catalysis* 52, (2009), 2041-2046
- [23] A.L. Kustov, M.Makkee, *Applied Catalysis B-Environmental*, 88, (2009) 263-271
- [24] J.P.A. Neeft, M.Makkee, J.A. Moulijn, *Fuel Proc. Tech.*, 47, (1996), 1.
- [25] *Eight Peak Index of Mass Spectra*, 3rd ed., Unwin, Surrey, 1983.

- [26] I. Nova, L. Lietti, L. Castoldi, E. Tronconi, P. Forzatti, J. Catal. 239 (2006) 244–254.
- [27] A. Lindholm, N.W. Currier, E. Fridell, A. Yezerets, L. Olsson, Applied Catalysis B-Environmental 75 (2007) 78-87.
- [28] L. Cao, J.L. Ratts, A. Yezerets, N.W. Currier, J.M. Caruthers, F.H. Ribeiro, W.N. Delgass. Industrial & Engineering Chemistry Research (2008), 47(23), 9006-9017.
- [29] P. Forzatti, L. Castoldi, I. Nova, L. Lietti, E. Tronconi, Catalysis Today (2006), 117(1-3), 316-320.
- [30] W.S. Epling, J.E. Parks, G.C. Campbell, A. Yezerets, N.W. Currier, L.E. Campbell, Catalysis Today (2004), 96(1-2), 21-30.
- [31] C.W. Yi, J. Szanyi, Journal of Physical Chemistry C 113 (2009) 2134-2140.
- [32] G. Zhou, T. Luo, R.J. Gorte, Applied Catalysis B-Environmental 64 (2006) 88-95.
- [33] M. Piacentini, M. Maciejewski, A. Baiker, Applied Catalysis B-Environmental 59 (2005) 187-195.
- [34] W.S. Epling, C.H.F. Peden, J. Szanyi, Journal of Physical Chemistry C 112 (2008) 10952-10959.
- [35] L. PerierCamby, G. Thomas, Solid State Ionics 93 (1997) 315-320.
- [36] N.W. Cant, M.J. Patterson, Catalysis Today 73 (2002) 271-278.

Table 1

| Dose time<br>→         | 60 s   |                              |                          | 300 s   |                              |                          | 600 s   |                              |                          |
|------------------------|--|------------------------------|--------------------------|---|------------------------------|--------------------------|---|------------------------------|--------------------------|
| Catalyst:<br>Soot<br>↓ | NO <sub>x</sub> desorbed<br>/ $\mu\text{mol g}^{-1}$ | T <sub>initial</sub><br>/ °C | T <sub>max</sub><br>/ °C | NO <sub>x</sub><br>desorbed<br>/ $\mu\text{mol g}^{-1}$ | T <sub>initial</sub> /<br>°C | T <sub>max</sub><br>/ °C | NO <sub>x</sub><br>desorbed<br>/ $\mu\text{mol g}^{-1}$ | T <sub>initial</sub> /<br>°C | T <sub>max</sub><br>/ °C |
| ∞                      | 131 (9%)   | 440                          | 550                      | 402 (27%)   | 350                          | 480                      | 521 (35%)   | 380                          | 520                      |
| 50:1                   | 40 (3%)  | 350                          | 460                      | 104 (7%)  | 330                          | 460                      | 133 (9%)  | 332                          | 460                      |
| 20:1                   | 67 (5%)  | 350                          | 465                      | 145 (10%)   | 330                          | 460                      | 156 (11%)   | 330                          | 450                      |
| 10:1                   | 62 (4%)  | 355                          | 470                      | 122 (8%)  | 325                          | 460                      | 137 (9%)  | 330                          | 460                      |
| 5:1                    | 20 (1%)  | 350                          | 480                      | 76 (5%)   | 345                          | 470                      | 177 (12%)   | 320                          | 450                      |

Table 1 showing absolute amounts of NO<sub>x</sub> desorbed and the temperature of maximum NO<sub>x</sub> desorption following a dose of 1%Pt / 10% BaO / Al<sub>2</sub>O<sub>3</sub> catalyst with NO (2000 ppm) + O<sub>2</sub> (10%) for various times with different catalyst : soot ratios. The numbers in parentheses indicate the fraction of the BaO present on the catalyst that was utilized during the trapping.



Figure 1

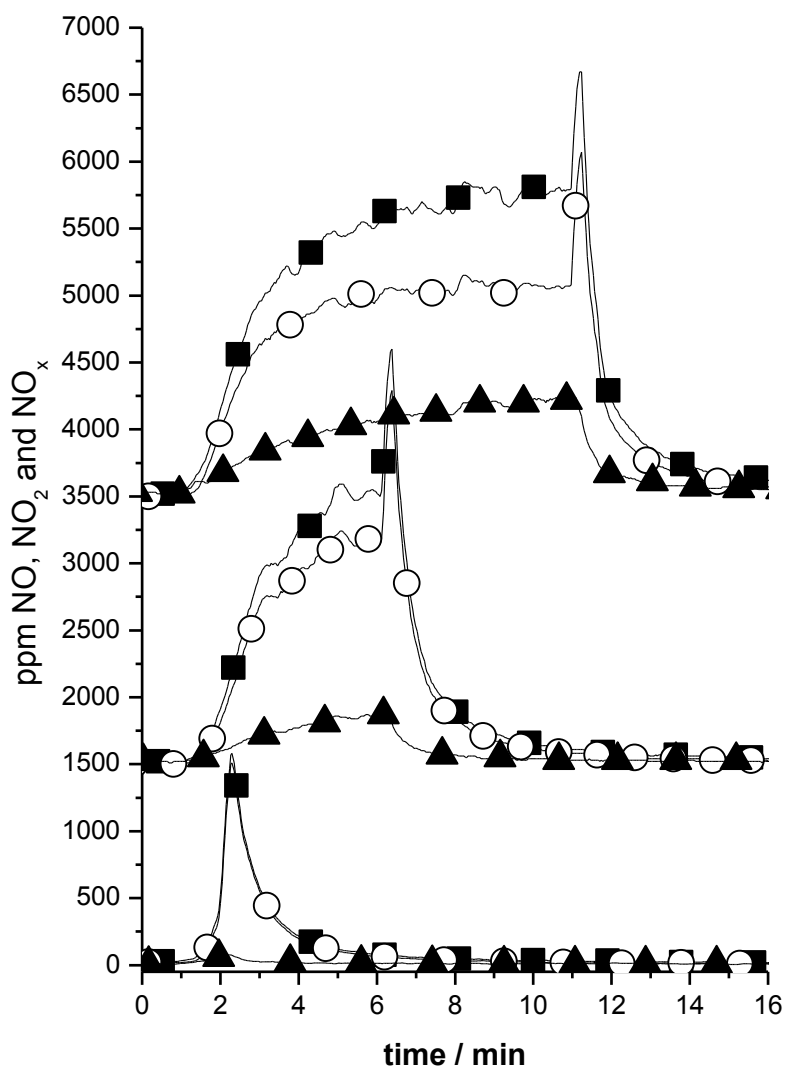


Figure 1. NO, NO<sub>2</sub> and NO<sub>x</sub> profiles during the dose (at 400 °C) of 1% Pt / 10% BaO / Al<sub>2</sub>O<sub>3</sub> with NO (2000 ppm) + O<sub>2</sub> (10%) for 60 s (lower plots), 300 s (middle plots) and 600 s (upper plots). NO (O), NO<sub>2</sub> (▲), NO<sub>x</sub> (■)

In all cases the NO + O<sub>2</sub> was switched into the stream at 1 min. Once the NO + O<sub>2</sub> is removed from the stream the catalyst is cooled to 200 °C – a process that takes ~ 10 minutes.

Figure 2

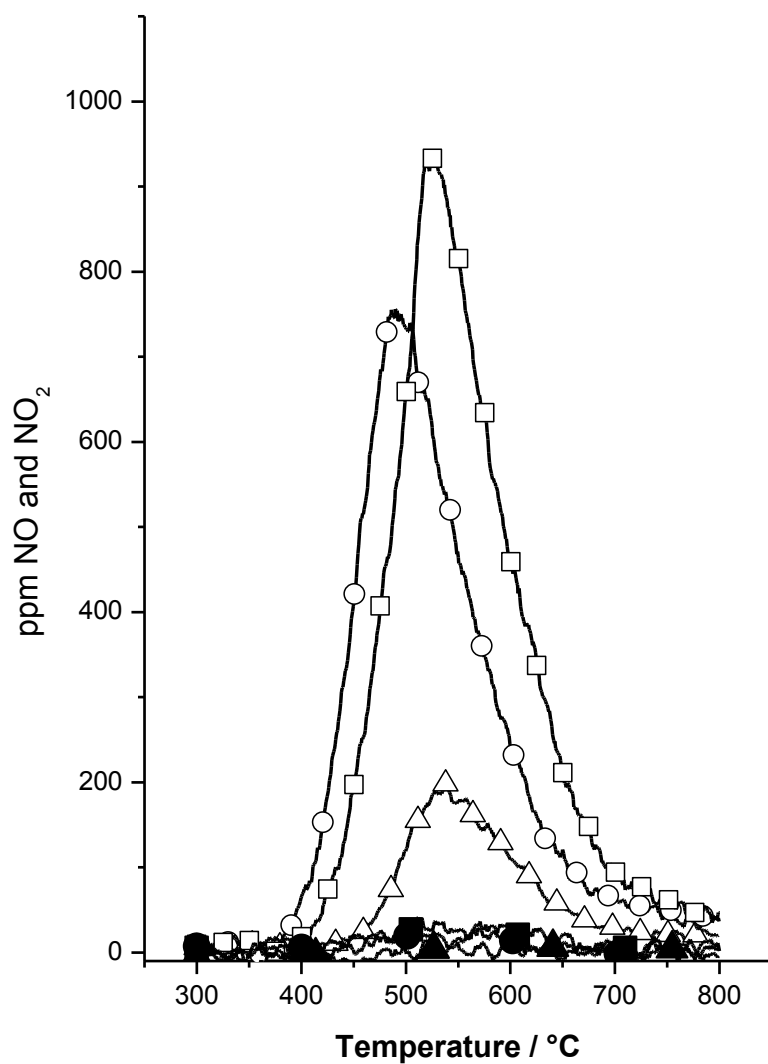


Figure 2. Temperature Programmed Desorption profiles following the NO + O<sub>2</sub> treatments detailed in Figure 1. NO – empty symbols, NO<sub>2</sub> – filled symbols. Dose times - 60 s ( $\Delta$ ,  $\blacktriangle$ ), 300 s ( $\circ$ ,  $\bullet$ ), 600 s ( $\square$ ,  $\blacksquare$ ). Samples were held in a flow of He while the temperature was ramped to 750 °C at 20 °C min<sup>-1</sup>.

Figure 3

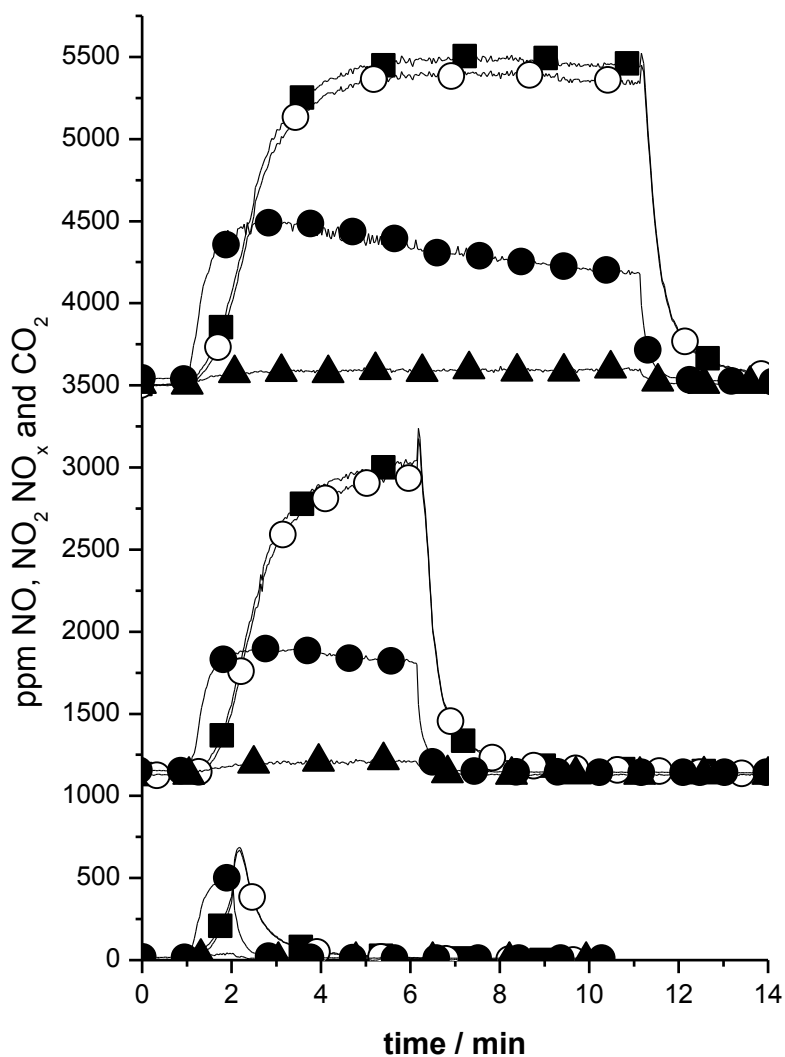


Figure 3. NO, NO<sub>2</sub>, NO<sub>x</sub> and CO<sub>2</sub> profiles during the dose (at 400 °C) of 50 mg 1% Pt / 10% BaO / Al<sub>2</sub>O<sub>3</sub> mixed with 5 mg of Printex U soot with NO (2000 ppm) + O<sub>2</sub> (10%) for 60 s (lower plots), 300 s (middle plots) and 600 s (upper plots). NO (○), NO<sub>2</sub> (▲), NO<sub>x</sub> (■), CO<sub>2</sub> (.). In all cases the NO + O<sub>2</sub> was switched into the stream at 1 min.

Figure 4

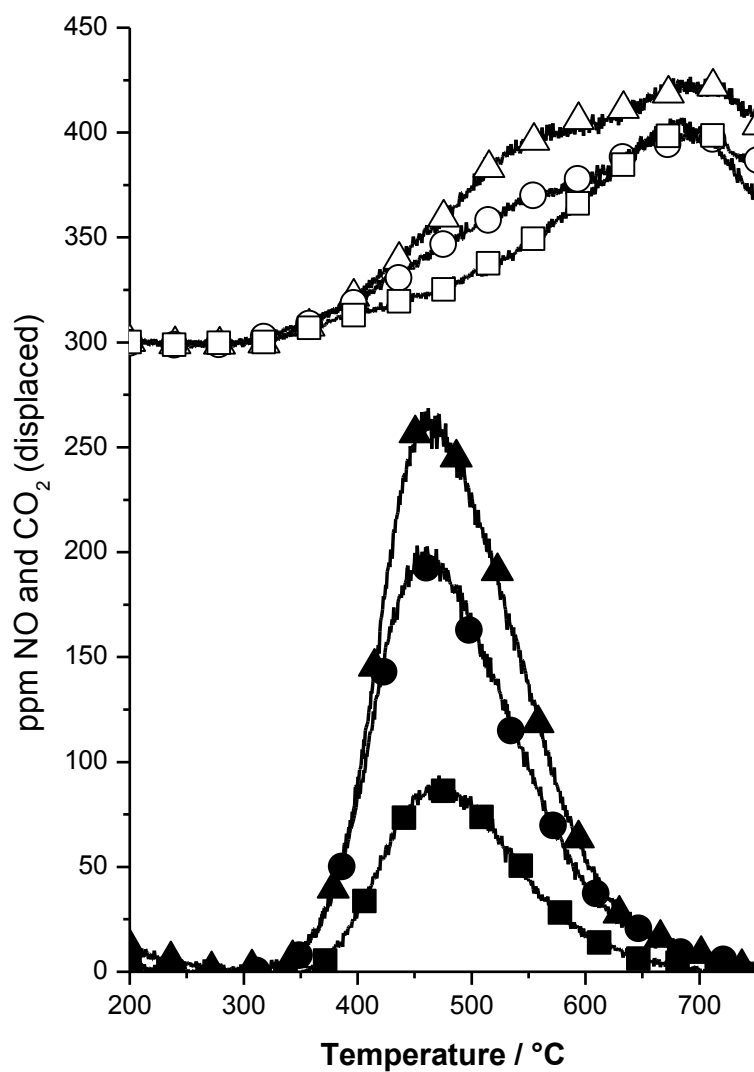


Figure 4. NO (closed symbols) and CO<sub>2</sub> (open symbols - displaced) profiles during TPD following the dose shown in Fig 3. Samples dosed in NO + O<sub>2</sub> for 60 s (■, □), 300 s (●, ○) and 600 s (▲, △).

Figure 5

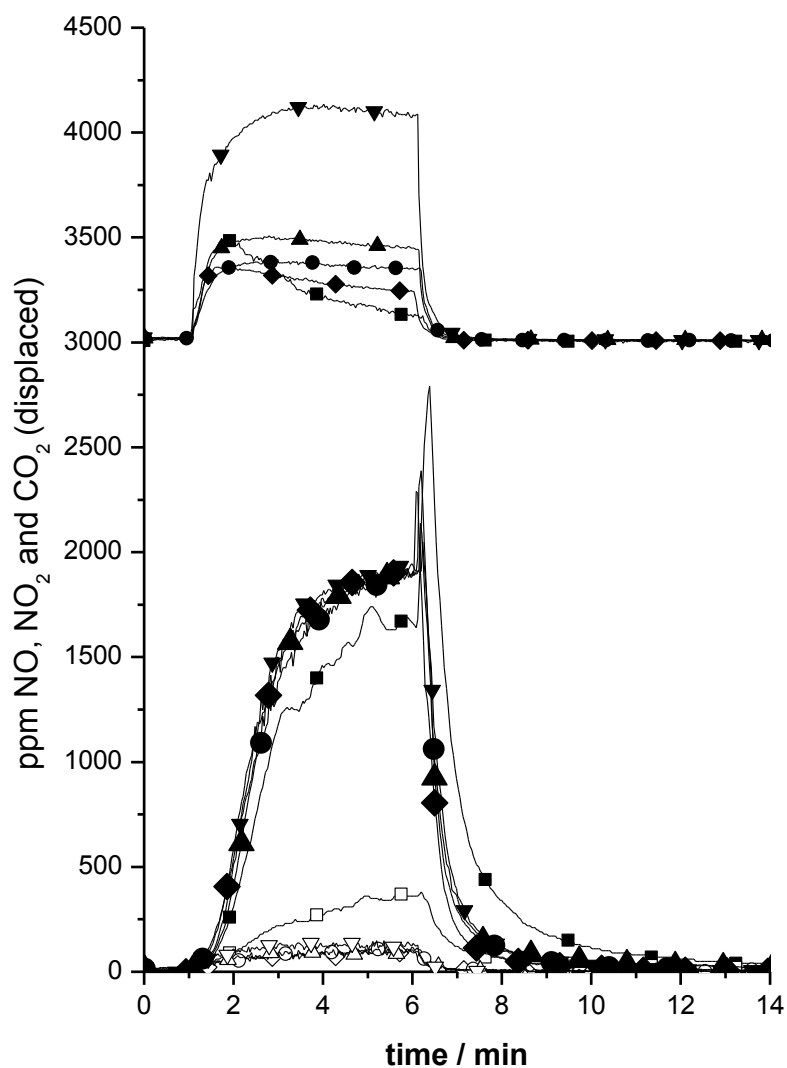


Figure 5. NO and CO<sub>2</sub> (closed symbols) and NO<sub>2</sub> (open symbols) profiles during the dose of a mixture of 50 mg 1% Pt / 10% BaO / Al<sub>2</sub>O<sub>3</sub> and 0 (■, □), 1 (◆, ◇), 2.5 (●, ○), 5 (▲, △) and 10 (▼, ▽) mg Printex U soot with NO (2000 ppm) + O<sub>2</sub> (10%) for 300 s. For clarity the CO<sub>2</sub> profiles are displaced to the top of the plot. In all cases the NO + O<sub>2</sub> was switched into the stream at 1 min.

Figure 6

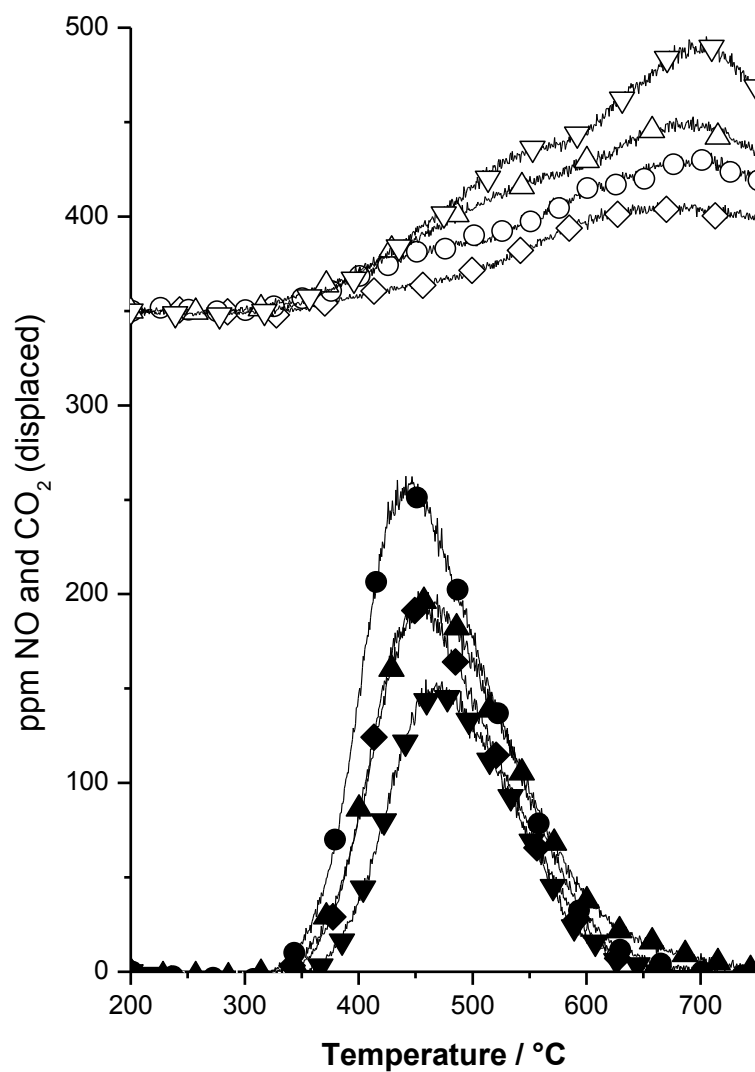
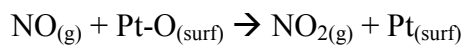
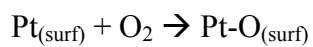
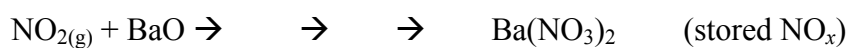


Figure 6. NO (closed symbols) and CO<sub>2</sub> (open symbols - displaced) profiles during TPD following the dose shown in Fig 5. 1% Pt / 10% BaO / Al<sub>2</sub>O<sub>3</sub> mixed with 1 (◆,◇), 2.5 (●,○) 5 (▲,△) and 10 (▼,▽) mg Printex U soot.

## Scheme 1

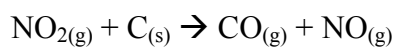


### Route 1



**or**

### Route 2



Scheme 1. Proposed mechanism for the  $\text{C}_{(\text{s})}$  poisoning of the  $\text{NO}_x$  trapping capacity of a 1% Pt 10% BaO  $\text{Al}_2\text{O}_3$  material.

## **Supporting information for**

### **The effect of C<sub>(s)</sub> on the trapping of NO<sub>x</sub> onto Pt Ba Al<sub>2</sub>O<sub>3</sub> catalysts**

James A Sullivan\* and Petrica Dulgheru,  
UCD School of Chemistry and Chemical Biology  
SFI SRC in Solar Energy Conversion,  
Belfield  
Dublin 4,  
Ireland



Figure S1

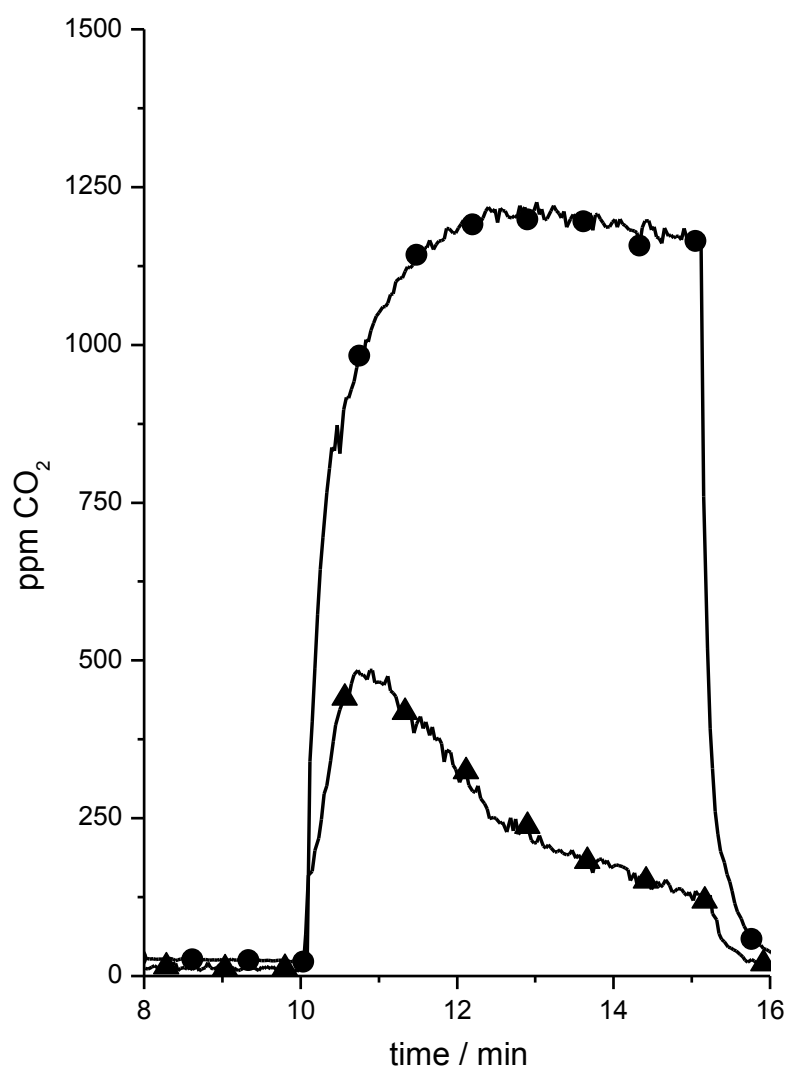


Figure S1. Plot showing CO<sub>2</sub> profiles following switch of NO + O<sub>2</sub> into the stream (for 300 s) at 400 °C over a Pt BaO Al<sub>2</sub>O<sub>3</sub> catalyst alone (●) and mixed with soot (catalyst:soot ratio = 10:1) (▲)

Figure S2

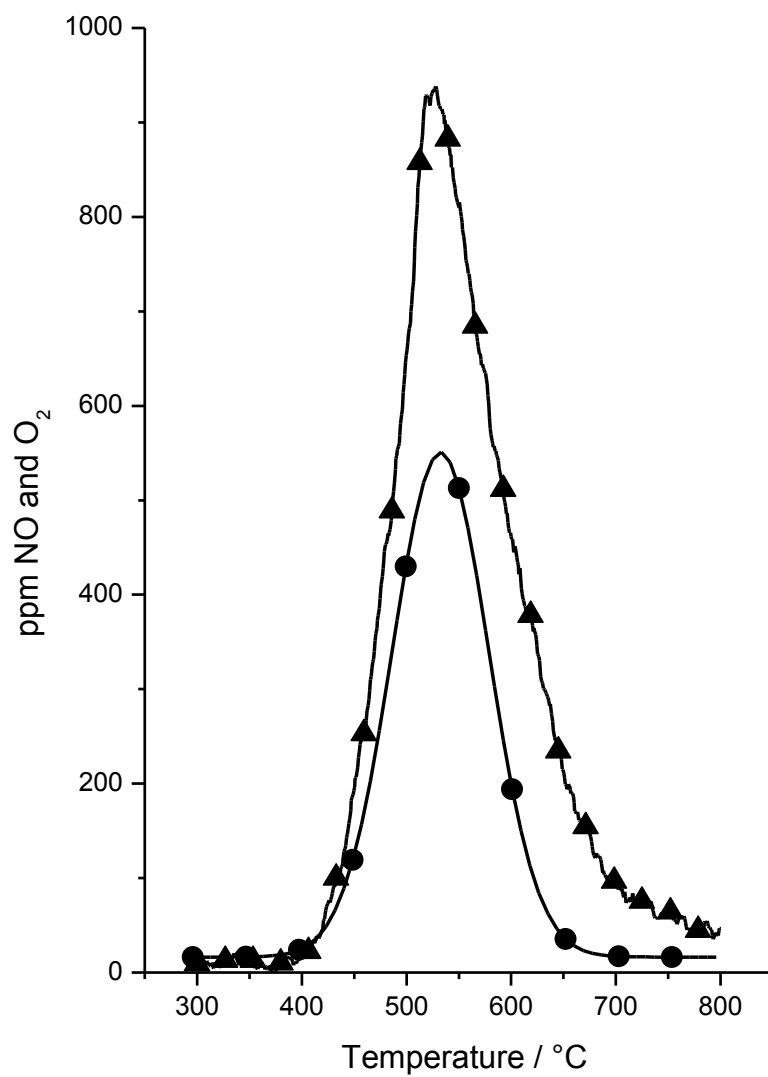


Figure S2. Plot showing typical NO (7) and O<sub>2</sub> (.) evolution during TPD. The example shown is from the material dosed for 600 s in the absence of C<sub>(s)</sub>.

Figure S3

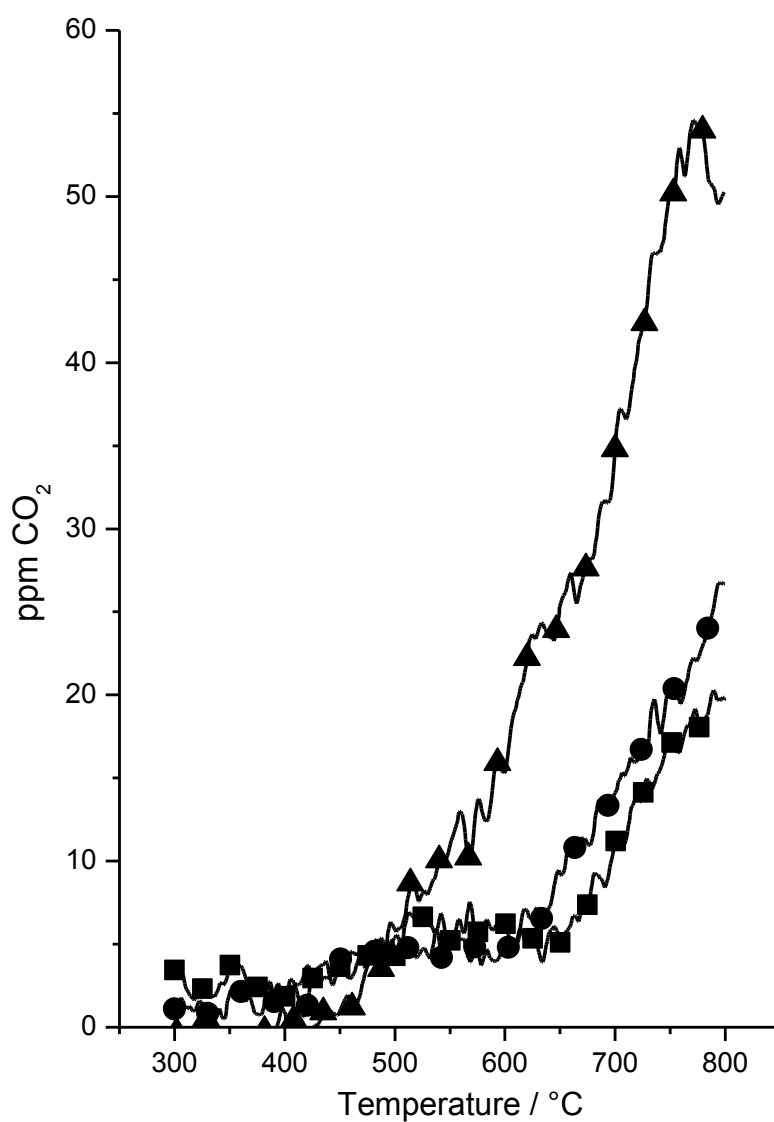


Figure S3. Plot showing CO<sub>2</sub> desorptions during TPD of the Pt BaO Al<sub>2</sub>O<sub>3</sub> catalyst which had been dosed in the absence of soot for 1 (Δ), 5 (●) and 10 (■) minutes. The amount of CO<sub>2</sub> liberated is significantly lower than in the equivalent experiments in the presence of soot.